ACS APPLIED MATERIALS & INTERFACES

RESEARCH ARTICLE

www.acsami.org

Real-Time Monitoring of Plasmonic Evolution in Thick Ag:SiO_2 Films: Nanocomposite Optical Tuning

José A. Jiménez,[†] Mariana Sendova,*[,†] and Marushka Sendova-Vassileva[‡]

[†]Division of Natural Sciences, New College of Florida, Sarasota, Florida 34243, United States

[‡]CL SENES, Bulgarian Academy of Sciences, 72 Tzarigradsko Chausee, 1784 Sofia, Bulgaria

ABSTRACT: An in situ optical microspectroscopy study of the surface plasmon resonance (SPR) evolution of Ag nanoparticles (NPs) embedded in thick SiO_2 films deposited on soda-lime glass has been conducted during thermal processing in air. The temperature and time dependences of the SPR were analyzed in the context of Mie extinction and crystal growth theories and were discussed along with consideration of oxidation processes and film/substrate physicochemical interactions. At relatively high temperatures, Ag NPs were indicated to grow first through a diffusion-based process and subsequently via Ostwald ripening. At lower temperatures, an initial decrease in Ag particle size was indicated due to oxidation, followed by NP diffusion-based growth. The growth and oxidation stages appeared temperature and time dependent, allowing for the tuning of material properties. The product of Ag NP oxidation was revealed by photoluminescence spectroscopy performed ex situ as single Ag^+ ions. The oxidative effect of the air atmosphere on Ag NPs was shown to be ultimately circumvented by the thick nanocomposite film. The phenomenon was explained on the basis of the displacement of the Ag/Ag^+ redox equilibrium toward Ag NP stability after ion migration toward the substrate being self-constrained. In addition, the current spectroscopic approach has been proposed for estimating the activation energy for silver diffusion in the SiO_2 matrix.

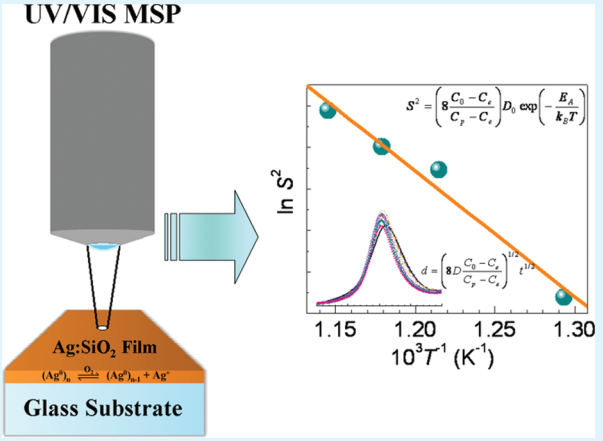

KEYWORDS: nanoparticles, optical absorption, photoluminescence, silver, sputtering, surface plasmon resonance

1. INTRODUCTION

Metal dielectric nanocomposites have been the subject of increasing interest because of their prospective utilization in the field of photonics.[1−8] Herein, a main feature is the surface plasmon resonance (SPR) exhibited by the metallic nanoparticles (NPs), which results from the collective oscillations of conduction band electrons in the metal.[3] The high local fields associated with the metal NPs near the SPR have made these nanostructures particularly desirable for applications in ultrafast nonlinear optics.[1,3,9−11] Thin metal nanocomposite films appear especially attractive for integrated optics applications because they are able to incorporate a large concentration of NPs by a variety of well-developed deposition methods and are compatible with solid-state optoelectronic technology.[7,12,13] Potentially useful in the material preparation ground is the magnetron sputtering technique, which has been shown to produce metal nanocomposite films having desirable large third-order nonlinear susceptibilities, $\chi^{(3)}$, due to the large particle volume fractions achieved.[12,13]

A critical issue for technological applications is the need for a thorough understanding of the dependence of material optical properties on processing parameters.[10,11,14−17] In this regard, considerable attention has been given to Ag NPs embedded in amorphous silica as promising nanocomposites and the dependence of material optical properties with heat treatment (HT) conditions including the atmosphere.[14−16,18] However, despite the importance for optical device applications, the current understanding of the relationship of processing parameters with particle formation and growth processes in connection with metal transport in Ag:SiO_2 nanocomposite films is still limited. Especially valuable in this respect would be a real time nondestructive monitoring of metal NP evolution during thermal processing. In fact, in situ optical characterization techniques can prove to be an efficient way for gaining control over material characteristics.[17,20] Moreover, coupling in situ optical monitoring with microscopic capabilities is highly desirable in order to overcome the disadvantage of traditional methods of averaging information over large sample volumes.[17,21] Recently, such an in situ optical microspectroscopy study was proposed by the authors[22] and applied to the study of the temperature and time dependences of NP growth and oxidation in thin (∼55 nm) Ag:SiO_2 nanocomposite films deposited on a soda glass substrate. Controlling the Ag/Ag^+ chemical equilibrium established in the matrix was also proposed. For instance, the detrimental effects of the oxidizing atmosphere were shown to be circumvented by applying an appropriate electric field during HT.[22] Yet, complete NP oxidation

Received: October 21, 2010
Accepted: January 10, 2011
Published: January 28, 2011

could not be prevented at high temperature in the absence of the field, and a quantitative determination of the activation energy for silver diffusion in the matrix was not achieved. In this work, the real time evolution of the SPR band of relatively thick (~800 nm) Ag:SiO_2 nanocomposite films deposited on soda glass substrates is studied during HT in air by the in situ optical microspectroscopy technique. Silver NP growth and oxidation processes are followed by analyzing the SPR in the context of Mie extinction and crystal growth theories. Furthermore, the discussion of the particle growth mechanisms serves as a basis for proposing an efficient, purely spectroscopic method for estimating the activation energy for silver diffusion in silica, based on the analysis of an appropriate set of isothermal time-dependent characteristics of the SPR. For the first time, to the best of our knowledge, such determination is carried out for Ag:SiO_2 films by application of the proposed technique in air atmosphere. Finally, it is pointed out how the detrimental effects of the atmosphere are ultimately overcome by use of the thick SiO_2 films serving as the Ag NP embedding matrix, based on the Ag/Ag^+ redox equilibrium and the influence of the substrate. It is also worth mentioning that identification of the product of Ag NP oxidation is performed ex situ by photoluminescence spectroscopy in order to assist in resolving the current controversy regarding the products of oxidation of matrix-embedded Ag NPs.[18]

2. EXPERIMENTAL SECTION

Silver-doped SiO_2 films were deposited on commercially available soda-lime glass substrates by magnetron cosputtering as described elsewhere.[23] The present study was carried out on films about 800 nm thick with a Si:O 1:2 stoichiometry and 2.50 atom % of Ag as determined by Rutherford backscattering spectroscopy. A CRAIC Technologies QDI 2010 UV/vis microspectrophotometer (MSP) equipped with a Linkam THMS600 temperature control stage was used to conduct in situ optical absorption measurements during HT at different temperatures in air. All samples were heated at a rate of 50 °C/min. Optical absorption measurements were performed with a 10X objective on 50 μm × 50 μm sample areas with particular attention given to keep sample position and conditions constant during experiments. Prior to data collection at a fixed temperature, the MSP objective was positioned and focused on the corresponding substrate for a reference scan. Thereafter, the objective was removed from the substrate, positioned on the sample, and focused on a particular area, where it remained for the entire period of data collection. Maintaining a fixed sample position during data collection was deemed critical because inspection of "as prepared" films at room temperature resulted in spectra that differed both in full-width at half-maximum (FWHM) and peak intensity of the SPR in association with particle size distribution.[24] For instance, shown in Figure 1 are room-temperature spectra corresponding to four different areas from an "as prepared" film for which Ag NP diameters of 1.98, 2.24, 2.50, and 2.66 nm were estimated by the method indicated below.

Particle size estimation was achieved by fitting experimental data on SPR absorption in the 2.0−4.0 eV region to theoretical spectra generated on the basis of the quasi-static (dipole) approximation of Mie theory.[25] Herein, the extinction cross-section σ_{ext} (equal to the absorption cross-section in this case) of a particle with radius R is expressed as

$$\sigma_{ext}(R, \omega) = \frac{9\omega}{c}\varepsilon_d^{3/2}\frac{4\pi R^3}{3}\frac{\varepsilon_2(\omega)}{[\varepsilon_1(\omega)+2\varepsilon_d]^2+\varepsilon_2(\omega)^2} \quad (1)$$

where ω is the angular frequency of the incident light, c is the speed of light in vacuum, and ε_d and $\varepsilon(\omega) = \varepsilon_1(\omega) + i\varepsilon_2(\omega)$ are the dielectric constants of the matrix and the metal, respectively. The dependence of metal dielectric function on particle size is further taken into account according to the formula proposed by Hövel et al.[26]

$$\varepsilon(R, \omega) = \varepsilon_{bulk}(\omega) + \frac{\omega_p^2}{\omega^2+i\omega\gamma_0} - \frac{\omega_p^2}{\omega^2+i\omega(\gamma_0+\beta v_F/R)} \quad (2)$$

where ω_p, v_F, and γ_0 are the plasma frequency, Fermi velocity, and relaxation frequency of the metal, respectively, and β is a phenomenological parameter that depends on details of scattering processes, equal to 1 for spherical Ag particles in silica.[25,26] The optical extinction coefficient α of the nanocomposite (equal to the absorption coefficient in the present study) is

$$\alpha = \sigma_{ext}N \quad (3)$$

where N is the particle concentration. The optical density (absorbance) of the film is the experimentally measured quantity (Figure 1) equal to the product of the thickness of the film and the absorption coefficient. As a result of the fitting procedure, an effective particle size was estimated (also referred to as "optical" size). Furthermore, according to eqs 1 and 3, the absorption peak intensity of the SPR band is directly related to the size of the particles and their concentration in the nanocomposite. Therefore, by following the evolution of the particle size obtained from the fits together with the SPR peak intenisty, conclusions can be drawn regarding the particle growth mechanisms. The significance of the spectroscopic approach for studying the nanocomposites in real time during HT is substantiated by the inherent difficulty of measuring particle size and concentration by any direct imaging method. Moreover, good agreement between optical characterization and transmission electron microscopy has been previously attained.[23,25] The basic assumptions of the NPs being spherical, much smaller than the wavelength of light and being far enough from each other so electrodynamic interactions between them can be neglected, have been also shown to be satisfied in similar samples.[23,25] An additional parameter estimated from the fitting with theoretical spectra is the refractive index of the matrix $n = (\varepsilon_d)^{1/2}$ due to sensitivity of the SPR peak position to optical properties of the host material.[7,27]

Photoluminescence spectroscopy was carried out ex situ with a Photon Technologies International spectrofluorometer for the purpose of identifying the silver species resulting from oxidation during thermal processing.

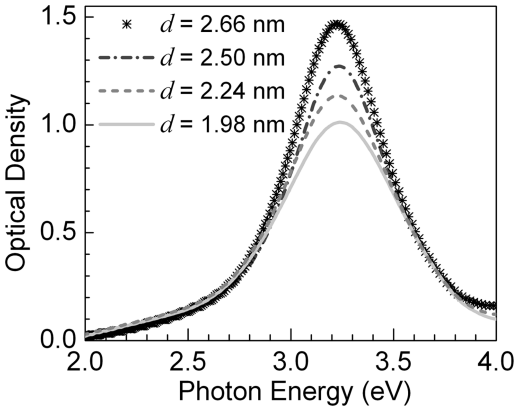

Figure 1. Absorption spectra for different areas of "as prepared" Ag:SiO_2 film at room temperature; corresponding estimated particle diameters d are displayed.

3. RESULTS AND DISCUSSION

Panel (a) and (b) of Figure 2 are representative absorption spectra that correspond to data collected during HT at 500 and

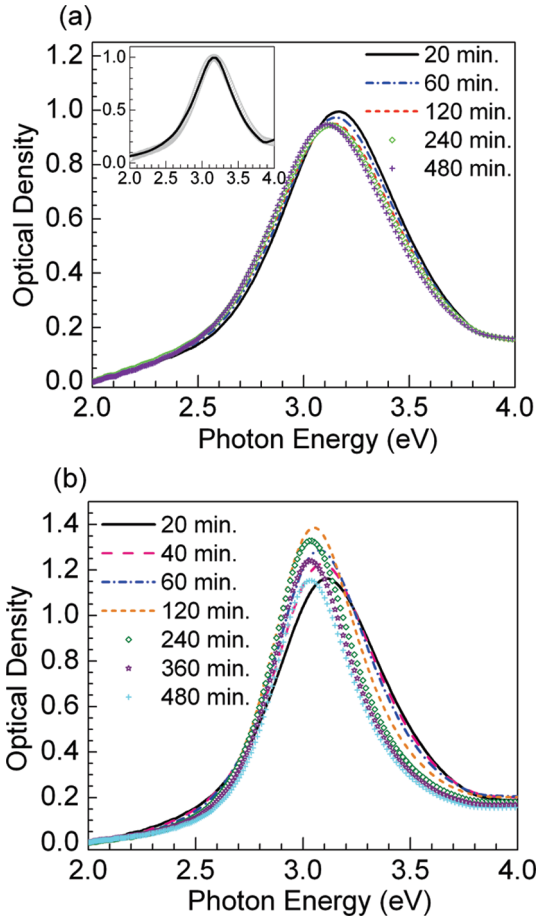

Figure 2. Absorption spectra of Ag:SiO_2 films during HT at (a) 500 °C and (b) 600 °C for displayed holding times in minutes. The inset in panel (a) shows the fit of the absorption spectrum of the sample after HT at 500 °C for 20 min (circles), with that calculated from the Mie theory with an estimated particle diameter of 2.20 nm (solid curve).

600 °C, respectively, at displayed holding times in minutes. The inset in panel (a) of Figure 2 shows a typical result for the fit of the experimental SPR absorption band with that calculated from the Mie theory,[25] in this case, corresponding to a particle diameter of 2.20 nm. From the numerical simulations and fitting to the experimental data, a tendency toward an increase in the matrix refractive index with increasing temperature and holding time was indicated by the SPR peak shift. Likely causes for this are related to the HT atmosphere, namely film densification,[28,29] and sodium doping of the film by the substrate because of an ion-exchange process promoted after silver oxidation.[29−31] Further experiments currently in progress in our group have shown that under a nitrogen atmosphere the SPR peak position remains practically unchanged during HT at fixed temperature.[31] Such results are consistent with the shift in the SPR peak position being related to variation in the local dielectric constant around the NPs in the matrix in association with oxygen diffusion during HT in air. Thus, a size dependent SPR peak shift can be excluded herein, in agreement with the NP size estimation within the dipole regime of the Mie theory.[24,25] In general, SPR peaks of samples studied during HT herein were observed to shift from around 3.17 to 3.04 eV, with associated fitting-deduced refractive indexes estimated between 1.36 and 1.53, respectively. More specifically, at 500 °C, the SPR peak position was observed to shift from 3.17 to 3.11 eV between 20 min and 480 min of HT in correspondence with estimated refractive indexes between 1.36 and 1.40, respectively. At 600 °C, the SPR peak position after 20 min of HT appeared at 3.11 eV, with an associated refractive index of 1.42, whereas a maximum refractive index was estimated at 1.53 in association to an SPR peak around 3.04 eV after 180 min.

Estimated particle "optical" diameters as a function of holding time at fixed temperature are presented in panel (a) of Figure 3, while panel (b) shows corresponding optical densities of SPR peaks. Overall, the estimated particle size evolution was observed to correlate with the evolving FWHMs of SPR bands, i.e., the particle size increases were accompanied by band narrowing, while particle size decreases showed together with band broadening, as expected for the quasi-static regime of the Mie theory.[24] For HT at 600 °C, NP size is indicated to increase steadily. However, two growth rates are apparent: a first fast rate shows initially for two hours, followed by a slower rate extending afterward for six more hours. Conversely, for the lower temperatures studied, i.e., from 500 to 575 °C, a decrease in particle size is initially observed, followed by particle growth. It is noticed that the lower the temperature, the longer the time period showing the NP size decrease. The subsequent NP growth observed at these temperatures appears steady. However, two growth rates become again discernible for HT at 575 °C: a first fast rate from about one to five hours, followed by a slower rate extending afterward from five to eight hours. By comparison with the trends in the experimental data in panels (a) and (b) of Figure 3, it becomes evident that the Ag NP size decrease is accompanied by a decrease in SPR peak absorption. On the other hand, the initial growth stage shows with an increase in SPR peak intensity, whereas the subsequent growth stage, where observed, is accompanied by a decrease in the SPR peak intensity. Thus, the observed correlation between estimated size and optical density allows for the assessment of growth processes discussed below.

Particle Growth. Let us first consider the process of Ag NP growth. The growth process appears favored at high temperatures because, for HT at 600 °C, a particle size increase was indicated continuously from the very beginning (Figure 3a). On the other hand, for temperatures lower than 600 °C, the particles appeared growing only after a certain holding time. The temperature dependence becomes further manifest from the fact that the initial size for HT at 600 °C is estimated between those for HT at 500 and 575 °C, temperatures for which particle size reduction was indicated prior to growth. Therefore, the evolution of the particle size in this narrow size range can be considered independent of the initial particle size.

According to the nucleation and growth theory, the three stages associated with particle formation and growth are the nucleation phase, diffusion-based growth which occurs at large supersaturation values, and the Ostwald ripening or recondensation stage, where larger particles grow at the expense of the dissolution of smaller ones.[32] In sputtered samples, the nucleation step occurs primarily during sample preparation, which becomes evident from the fact that SPR absorption was observed in samples prior to any HT (Figure 1). However, together with stable nuclei and small particles, the sputtering process may result in the presence of "dissolved" Ag atoms (or unstable few-atom clusters) and large supersaturation values. Under such circumstances, diffusion-based growth takes place at elevated temperatures in order for the supersaturation to be decreased, leading to an increase in particle size without a change in particle concentration. During this process, the average particle diameter

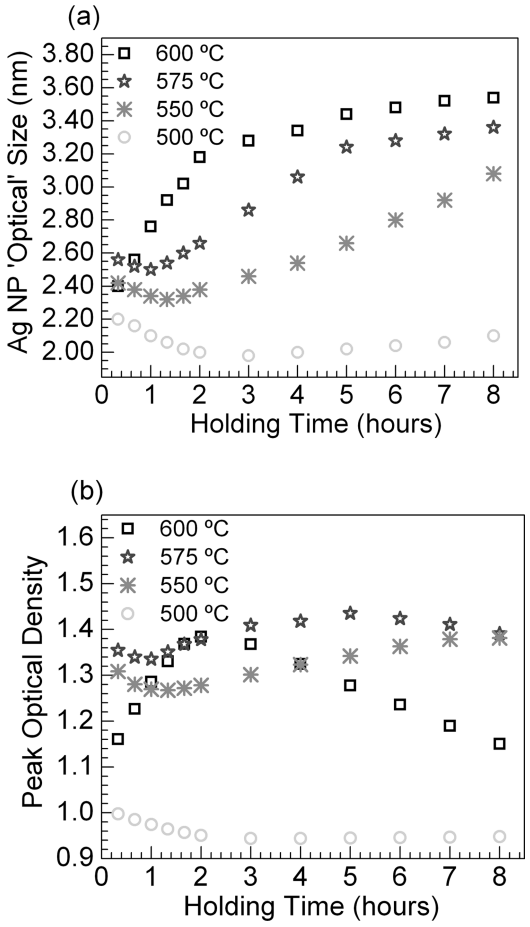

Figure 3. (a) Evolution of Ag NP "optical" size (diameter) and (b) SPR peak absorption with the holding time for Ag:SiO_2 films during HT at displayed temperatures.

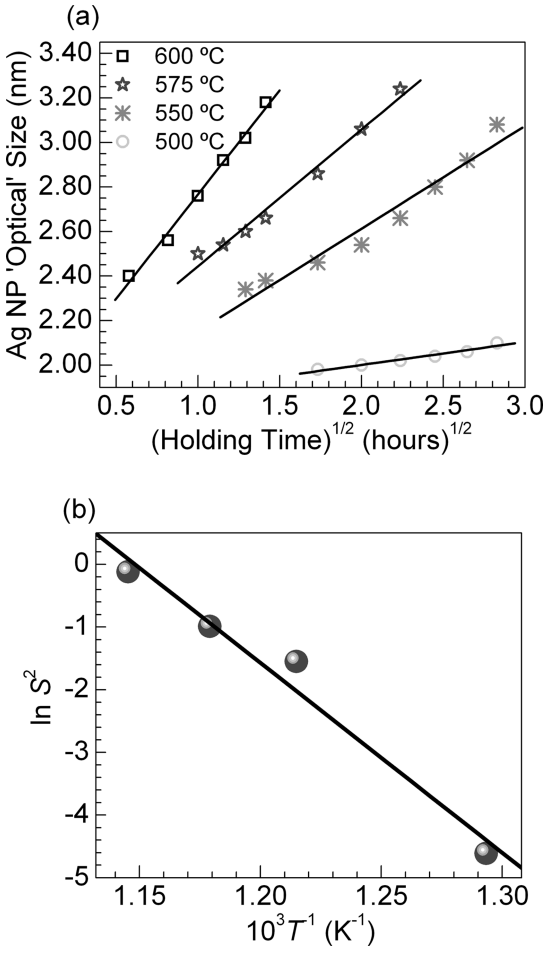

Figure 4. (a) Variation of Ag NP "optical" size (diameter) with $t^{1/2}$ corresponding to the early growth phase during HT at displayed temperatures. Solid lines are linear fits to data (discussed in text). (b) Plot of natural logarithm of the square of slopes determined from linear fits of data in (a) vs reciprocal absolute temperature (ln S^2 vs T^{-1}).

d varies linearly in proportion to the square root of the holding time t as

$$d = \left(8D\frac{C_0 - C_e}{C_p - C_e}\right)^{1/2} t^{1/2} \quad (4)$$

where C_0 is the initial concentration of limiting reactant Ag in the matrix, C_e is the equilibrium concentration in the matrix at a fixed temperature T, C_p is the concentration of reactant in the particle, and

$$D = D_0 \exp\left(-\frac{E_D}{k_B T}\right) \quad (5)$$

is the diffusion coefficient where k_B is Boltzmann constant, D_0 is the diffusion constant, and E_D is the associated activation energy.[32] Spectroscopically, such a growth mechanism would result in an increase in SPR peak intensity simultaneous with the band narrowing because in the quasi-static regime of the Mie theory, the extent of absorption is directly proportional to particle size.[24,33] This in effect becomes evident from data in Figure 3. The increase in Ag NP size in the first two hours during HT at 600 °C is accompanied by an increase in SPR absorption. Such correspondence is also evident for the following periods of HT: from 1 to 5 h at 575 °C, from 80 min to 8 h at 550 °C, and from 3 to 8 h at 500 °C. Moreover, the variation of Ag NP size with $t^{1/2}$ during the time periods considered for the four different temperatures is further apparent from panel (a) of Figure 4. Therefore, the data suggests that the early stage of Ag NP growth occurs via Ag atom diffusion to particle surface in the supersaturated solid matrix. From linear fits to the data in panel (a) of Figure 4, increasing slopes S of 0.10 nm/h$^{1/2}$, 0.46 nm/h$^{1/2}$, 0.61 nm/h$^{1/2}$, and 0.94 nm/h$^{1/2}$ are estimated for 500, 550, 575, and 600 °C, respectively, indicating an increase in the particle growth rate with temperature. From eqs 4 and 5, the square of the obtained slopes is expressed as

$$S^2 = \left(8\frac{C_0 - C_e}{C_p - C_e}\right) D_0 \exp\left(-\frac{E_D}{k_B T}\right) \quad (6)$$

which can be rearranged as

$$\ln S^2 = \left(-\frac{E_D}{k_B}\right)\frac{1}{T} + \ln Q \quad (7)$$

where $Q = 8D_0(C_0 - C_e)/(C_p - C_e)$. Therefore, a plot of ln S^2 vs T^{-1} allows for a direct estimation of the activation energy for Ag diffusion in the growth regime. Such a plot is presented in panel

(b) of Figure 4, where from the slope of the linear fit to the data, an apparent activation energy of diffusion, E_D, of 2.6 eV is estimated. Studies reporting activation energies for Ag diffusion in SiO_2 films in association to NP growth or diffusion driven by concentration gradients are scarce. However, there are reports on Ag diffusion in various glassy bulk matrices, where the values for the activation energies associated with the early growth stage distinguished by large supersaturation have been observed to vary widely, namely from about 0.28 to 5.1 eV.[17,34,35] Thus, the Ag diffusion activation energy appears largely dependent on the physicochemical properties of the matrix. Still, a contribution to the value estimated herein from an additional energy barrier imposed by the oxidation process going in parallel with the diffusion-based growth cannot be excluded. Additional experiments currently in progress are expected to shed more light onto this contribution. It should be noted that in ref 22 no diffusion-based growth was observed for the thin silica films during HT in air, even though the silver concentration was almost two times larger. Apparently, the diffusion of atmospheric oxygen within the thinner film prevented the progress of such a growth stage by consuming "dissolved" Ag atoms, thereby decreasing the supersaturation rapidly. Hence, the relatively thick films effectively overcome the detrimental effects of the oxidizing air atmosphere even at rather low Ag concentrations, so diffusion-based Ag particle growth in the supersaturated solid solution is manifested. The oxidation process associated with the NP size decrease estimated initially from 500 to 575 °C (Figure 3a) shall be later discussed, following the forthcoming discussion of the second stage of NP growth.

During the ripening stage, the degree of supersaturation, $(C_0 - C_e)$ becomes low and particle size increases, while particle concentration decreases due to dissolution of smaller particles.[32] As a consequence of the progress of this process, a broadening in the particle size distribution is expected. Nevertheless, nanosized particles are known to dominate the dipole absorption, while subnanometric ones undergoing dissolution become nonplasmonic in due course.[24] The spectroscopic outcome can therefore be such that growth may dictate the spectrum, i.e., the contribution of band narrowing to the SPR prevails over any broadening contributed by size dispersion. This is in fact what becomes evident from analyzed data shown in Figure 3: growth is still suggested after the conclusion of the diffusion-based growth indicated. Additionally, the SPR peak intensity in this growth regime would be affected by a competition between the following two processes (eqs 1 and 3): the particle size increase and the particle concentration decrease. The data presented in Figure 3 for 575 and 600 °C after five and two hours of HT, respectively, shows that even in the presence of a particle size increase, the SPR peak intensity decreases. Therefore, a drop in particle concentration concomitant with the growth process is suggested, which is in agreement with the Ostwald ripening mechanism. If Ag NP growth occurred herein through the diffusion-based mechanism, the concentration of growing particles would remain unaffected, and the preceding trend of increase in the SPR peak absorption (vide supra) would prolong, which is clearly not the present case. Herein, a contribution to the Ag particle concentration decrease from oxidation cannot be ruled out (vide infra). However, the consistent correlation observed between optical density and estimated size allows confidence in the growth mechanism elucidation. Hence, even though a potential contribution from a broader size distribution to the SPR spectral shapes can not be excluded, the second stage of particle growth indicated can be considered to take place via the Ostwald ripening mechanism.

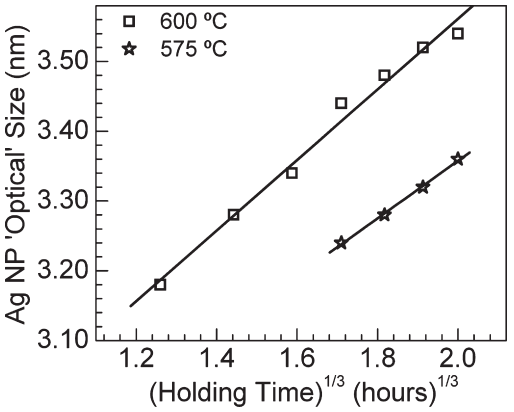

Figure 5. Variation of Ag NP "optical" size (diameter) with $t^{1/3}$ corresponding to the late growth phase during HT at displayed temperatures. Solid lines are linear fits to data (discussed in text).

Here, particle size varies linearly in proportion to the cube root of the holding time t as

$$d = \left(\frac{32\delta D}{9}\right)^{1/3} t^{1/3} \quad (8)$$

where δ is a coefficient related to interfacial surface tension.[32] Tanahashi et al.[19] conducted a study on the effects of HT on Ag NP growth for sputtered Ag:SiO_2 nanocomposite films and reported linear fits to data as

$$d = At^{1/3} + B \quad (9)$$

in association with particle growth during ripening. They found a value for A of 20.9 nm/h$^{1/3}$ indicative of a rapid growth for a sample with a large Ag concentration (28.0 at. %) at a HT temperature of 700 °C in air. In our case, the dependence of NP size on $t^{1/3}$ is observed for 575 and 600 °C after five and two hours of HT, respectively, from data plotted in Figure 5. From linear fits to the data, increasing slopes of 0.41 nm/h$^{1/3}$ and 0.51 nm/h$^{1/3}$ are estimated for HT at 575 and 600 °C, respectively, indicating a faster growth of Ag NPs at 600 °C. The slower growth of Ag NPs observed in our case relative to that reported by Tanahashi et al.[19] is possibly related to our Ag concentration being much smaller, the lower temperature employed herein, and the presence of competing processes discussed below. Concentration effects seem important because for the thin Ag:SiO_2 film having nearly twice the silver concentration of that studied herein, higher slopes of 1.2 and 2.0 nm/h$^{1/3}$ were estimated in association with Ostwald ripening during HT at 550 and 600 °C, respectively.[22] Thus far, the current results appear consistent with recent studies on glass-embedded Ag NPs, where particle growth has been ascribed first to a silver diffusion process followed by Ostwald ripening.[35,36]

Oxidation. Now that the particle growth mechanisms have been elucidated, let us consider the initial Ag NP size decrease observed at the lower temperatures studied. It has been previously considered by thermodynamic arguments that the oxidation of Ag NPs is favorable at low temperatures because of the more negative free energy change.[37] However, from the kinetics standpoint, an increase in the oxidation rate with temperature is expected, which makes the process substantial at relatively high temperatures. Data presented in Figure 3 appears consistent with

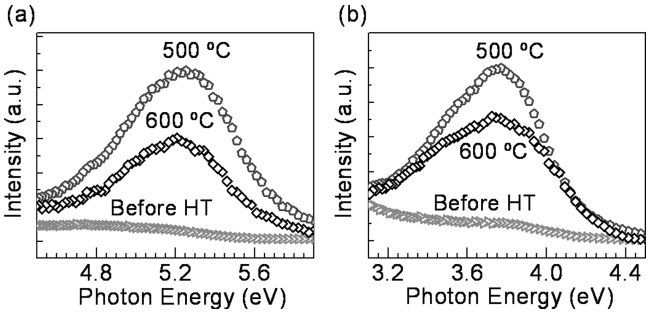

Figure 6. Photoluminescence of Ag:SiO_2 films before and after HT at 500 and 600 °C. Panel (a) shows excitation spectra for emission monitored at 3.70 eV (335 nm) and (b) shows emission spectra obtained under excitation at 5.28 eV (235 nm).

such considerations because a decrease in particle size initially extends to 180, 80, and 60 min for HT at 500, 550, and 575 °C, respectively. Moreover, consistent with the oxidation process, a decrease in SPR peak intensity is observed concomitantly with a decrease in NP size deduced from the SPR band fits. It is worth noting that the particle sizes estimated herein did not exceed the critical size for oxidation indicated by Bi et al.[37] of 4 nm in diameter, above which Ag NPs would become more stable against oxidation. In addition, an initial fast oxidation of metals has been previously reported in association with oxygen incorporation.[38] Herein, the samples are being submitted to HT in an air atmosphere, which makes the oxidation process likely at moderate temperatures due to oxygen diffusion.[15,39] It then seems likely that the current results are related to significant oxygen uptake during the early stages of HT. The question arises as to why the particle size decrease is followed by NP growth, but first the identity of the silver species resulting from Ag NP oxidation shall be elucidated.

The chemical and physical nature of silver after oxidation of matrix-embedded Ag NPs has been recently a controversial subject.[15,16,18,37,40] Bi et al.[37] reported the reversible oxidation and reduction of Ag NPs in mesoporous silica indicated by the vanishing and reappearance of the SPR. The authors explained the results in terms of the formation of an oxide layer around NPs due to successive oxidation. However, no direct evidence was reported in relation to the formation of silver oxide. Subsequent studies indicated that the oxidation of NPs did not result in the formation of Ag_2O but instead in single Ag^+ ions.[15,40] It was pointed out that in the case of mesoporous silica, Ag^+ ions are attached to dangling bonds on pore walls, whereas for soda-lime glasses an $Ag^+ \leftrightarrow Na^+$ ion-exchange takes place.[40] On the other hand, Pal and De[18] recently reported on the oxidation of Ag NPs in a silica film into silver oxides and the reversible reduction of silver into particles in a reducing atmosphere. It is noteworthy, however, that the authors observed photoluminescence spectra typical of radiative relaxation of single Ag^+ ions, and no such emission as that attributed to Ag_2O[41] was reported. Photoluminescence spectroscopy is well known for its reliability to reveal the chemical and physical states of ionic silver species consistently.[15,41−44] Other speculations for the existence of silver oxides as a result of Ag NP oxidation in silica have been reported,[14,29,30] but these lack relevant information on sample luminescence characterization. Accordingly, photoluminescence spectra shown in Figure 6 became crucial in the current elucidation of silver transformations upon HT. The lowest and highest temperatures were chosen for this assessment, i.e., 500 and 600 °C, as quite contrasting behaviors were observed from optical absorption results (vide supra). Excitation spectra of heat-treated samples presented in panel (a) of Figure 6 show an excitation band around 5.25 eV known to be characteristic of the Ag^+ luminescent centers because of the $4d^{10} \rightarrow 4d^9\ 5s^1$ parity-forbidden transitions, which are partially allowed in a solid due to coupling with host vibrations.[42−44] In fact, under excitation near the top of the aforementioned band at 5.28 eV (235 nm), the emission spectra shown in panel (b) of Figure 6 were recorded, which show broad bands for the samples after HT with a maximum around 3.75 eV (331 nm), also consistent with the presence of single Ag^+ ions.[42,43] Therefore, it becomes evident that Ag^+ optical centers result as a product of Ag oxidation and that the oxidation process occurred within the range of temperatures studied. The "as prepared" sample, in contrast, did not show the excitation and emission bands, which is indicative of negligible oxidation during the time of sample storage at room temperature in air atmosphere. The fact that oxidation was detected even where no spectroscopic indication of a NP size decrease was observed (HT at 600 °C, Figure 2a) is consistent with the size selectivity of the process,[45] i.e., atoms and small clusters are preferentially oxidized versus large NPs. At the same time, relatively large NPs may continue to grow due to diffusion of Ag atoms, which at high sample temperatures are able to compete successfully over oxidation. As to the possible presence of Ag_2O, no photoluminescence attributable to such a compound[41] was observed in our experiments, in agreement with the fact that Ag_2O is unstable at temperatures above 200 °C.[37]

The significant effect of the soda-lime glass substrate on NP oxidation should be also taken into account. Substrate effects on Ag/Ag^+ redox processes in Ag NPs have been studied by Hu et al.,[40] where a significant influence from soda-lime glass because of an $Ag^+ \leftrightarrow Na^+$ ion-exchange has been observed. In fact, an interdiffusion process between Ag^+ ions in doped silica films and Na^+ in soda-lime substrates was previously reported by Li et al.,[30] where the resulting content of sodium in the coating was suggested to increase matrix basicity as previously pointed out by Mennig et al.[29] Moreover, studies conducted by García et al.[43] on silver-doped silica coatings deposited on different substrates also showed that for soda-lime glasses, Ag^+ ions diffuse into the substrate, and this results in their stabilization in the glass network by interaction with nonbridging oxygen as indicated by the resulting photoluminescence. Recent investigations carried out in our group on thinner Ag:SiO_2 nanocomposite films on the same substrate have also shown consistent results in this respect.[22] In fact, photoluminescence spectra in Figure 6 closely resemble the results for the thin films studied without the influence of the applied electric field during HT.[22] Accordingly, Ag^+ diffusion into the substrate is more than likely in our case, which points toward the observed luminescence being largely due to Ag^+ ions incorporated in the soda-lime glass.

Let us now get back to the question as to why the particle size decrease is followed by NP growth even at the lowest temperature studied. The temperature dependence of the growth and oxidation processes appears related to the rates of involved competing processes, as already suggested in connection to oxidation at 600 °C. The diffusion of "dissolved" Ag atoms must compete successfully with oxidation in order for the limiting reactant Ag to reach existing particles and result in NP growth. This becomes especially important in dealing with low concentrations of silver, where the average distance that atoms travel becomes large. In such scenario, it seems that oxidation becomes initially dominant

at lower temperatures, whereas at the highest temperature of 600 °C, Ag diffusion competes successfully over the oxidation still occurring at this temperature as indicated by photoluminescence data. However, particle growth eventually dominates over oxidation even at the lowest temperature after sufficient holding time. The reason for this is believed to be related to the fact that the redox process is indeed a chemical equilibrium, which has also become evident from additional studies performed by our group on thinner Ag:SiO_2 nanocomposite films.[22] Thus, two likely causes arise which could influence the chemical stability of Ag NPs facilitating their further growth: (*i*) an increased density of the films resulting in a decreased oxygen uptake (a HT atmosphere effect), and (*ii*) a less efficient removal of silver ions by the substrate (a substrate effect). The former has been already suggested from the found tendency of the SPR peak to red shift, suggesting an increase in the refractive index of the films during HT. On the other hand, although oxygen incorporation may decrease with an increase in film density, oxygen diffusion in the SiO_2 matrix likely continues during HT as in fact has been suggested by the experiments on thin films where complete vanishing of the SPR was observed at 600 °C.[22] Thus, substrate effects seem more significant at this stage of the HT. Apparently, the efficiency of the removal of Ag^+ ions from the film diminishes during HT due to the relatively large thickness of the films studied. A similar result was in fact recently reported by Hu et al.[46] in a comparative study on Ag NP oxidation in thin and thick films on mesoporous SiO_2 prepared by thermal evaporation. The authors observed that Ag NPs were not completely oxidized during HT of the thick films in air, which was partially attributed to substrate saturation by Ag^+ ions.[46] Similarly, it can be considered herein that the near surface region of the soda glass substrate may become saturated with silver ions in the early stages of HT, therefore, suppressing the ion migration, which is necessary for sustained oxidation. Thereafter, the impaired removal of ions from equilibrium[22] would assist in preserving the supersaturation in the thick film and at the same time provide additional stability for the NPs, which may as a consequence participate in the diffusion-based growth. The fact that the higher the temperature the shorter the time period shows that the NP size decrease could be related to a highest oxidation rate with increasing temperature, which would imply a more rapid saturation of the surface layer of the substrate. Further assessments on the kinetics of NP oxidation in silica films are underway. As a final remark, it is also reasonable from this assessment to assume that the NPs grow via Ag atom diffusion to particle surface. Migration of silver ions toward the substrate involves their diffusion away from the particles in the film. Also, a chemical equilibrium implies that the ion concentration reaches a stable limit in association with the attained NP stability. Thus, the limiting reactant being steadily consumed during the growth is suggested to be the neutral silver atom, which is clearly the specie making the process manifest.

4. CONCLUSIONS

Real-time monitoring of plasmon resonace evolution in Ag NPs embedded in relatively thick SiO_2 films deposited on soda-lime glass has been conducted during HT in air. Data treatment in the context of Mie extinction and crystal growth theories, together with considerations on the oxidation process and substrate influence, has enabled a reliable assessment of Ag particle transformations for the system. Silver NPs were indicated to grow at high temperatures, first through a diffusion-based process and subsequently via Ostwald ripening. It was shown that the activation energy associated to Ag diffusion in the system can be estimated by the current technique nondestructively and in situ. The apparent activation energy associated to the diffusion-based Ag NP growth phase was determined from a set of isothermal time dependences of plasmonic evolution, yielding a value of 2.6 eV. This was possible because of the remarkable influence of film thickness, which allowed for the diffusion-based process to develop, in contrast to the thin film previously studied,[22] where only Ostwald ripening was manifested. At the lower temperatures studied, an initial decrease in Ag particle size was observed due to oxidation. The NP size decrease followed by NP growth was discussed in the framework of the redox equilibrium in the film being displaced in favor of Ag NP stability mainly due to less efficient ion removal by the substrate during the late phases of HT. Therefore, the detrimental effects of the air atmosphere, previously observed to prevail in thin films, can be overcome by the use of thicker SiO_2 films for Ag NP inclusion. The temperature and time dependences of the growth and oxidation stages in the thick film system allow for superior control over nanocomposite optical properties relative to the thin film system.[22] In terms of the product of oxidation, no indication of the presence of Ag_2O was observed. In contrast, Ag NP oxidation was found to generate single Ag^+ ions as revealed by photoluminescence spectroscopy.

The current report provides important insights to the tailoring of material optical properties for prospective applications in photonics. Additional experiments are underway concerning the in situ assessment of NP growth processes during thermal processing under an inert atmosphere. Another interesting aspect to further look at would be to quantitatively evaluate the energy barrier of the oxidation process itself.

AUTHOR INFORMATION

Corresponding Author

*Phone: 1-941-487-4384. Fax: 1-941-487-4396. E-mail: sendova@ncf.edu.

ACKNOWLEDGMENT

Financial support from ARL-W911NF-09-2-0004 is gratefully acknowledged. We thank Jean C. Pivin for the Rutherford backscattering spectroscopy analyses and Miguel A. García for the program code modeling Mie resonances.

REFERENCES

(1) Yamane, M.; Asahara, Y. *Glasses for Photonics*; Cambridge University Press: Cambridge, U.K., 2000.

(2) Maier, S. A.; Atwater, H. A. *J. Appl. Phys.* **2005**, *98*, 011101.

(3) Palpant, B. In *Non-linear Optical Properties of Matter*; Papadopoulos, M. G., Sadlej, A. J., Leszczynski, J., Eds.; Springer: Dordrecht, 2006.

(4) Fort, E.; Grésillon, S. *J. Phys. D: Appl. Phys.* **2008**, *41*, 013001.

(5) Jiménez, J. A.; Lysenko, S.; Liu, H. *J. Appl. Phys.* **2008**, *104*, 054313.

(6) Eichelbaum, M.; Rademann, K. *Adv. Funct. Mater.* **2009**, *19*, 2045–2052.

(7) Walters, G.; Parkin, I. P. *J. Mater. Chem.* **2009**, *19*, 574–590.

(8) Brongersma, M. L.; Shalaev, V. M. *Science* **2010**, *328*, 440–441.

(9) Liao, H.; Lu, W.; Yu, S.; Wen, W.; Wong, G. K. L. *J. Opt. Soc. Am. B* **2005**, *22*, 1923–1926.

(10) Yang, X.-C.; Dong, Z.-W.; Liu, H.-X.; Xu, J.-X.; Qian, S.-X. *Chem. Phys. Lett.* **2009**, *475*, 256–259.

(11) Jiménez, J. A.; Lysenko, S.; Vikhnin, V. S.; Liu, H. *J. Electron. Mater.* **2010**, *39*, 138–143.
(12) Tanahashi, I.; Yoshida, M.; Manabe, Y.; Tohda, T.; Sasaki, S.; Tokizaki, T.; Nakamura, A. *Jpn. J. Appl. Phys.* **1994**, *33*, L1410–L1412.
(13) Tanahashi, I.; Manabe, M.; Tohda, T.; Sasaki, S.; Nakamura, A. *J. Appl. Phys.* **1996**, *79*, 1244–1249.
(14) Babapour, A.; Akhavan, O.; Azimarad, R.; Moshfegh, A. Z. *Nanotechnology* **2006**, *17*, 763–771.
(15) Hu, J.; Lee, W.; Cai, W.; Tong, L.; Zeng, H. *Nanotechnology* **2007**, *18*, 185710.
(16) Hu, J.; Wang, L.; Cai, W.; Li, Y.; Zeng, H.; Zhao, L.; Liu, P. *J. Phys. Chem. C.* **2009**, *113*, 19039–19045.
(17) Jiménez, J. A.; Sendova, M.; Liu, H. *J. Lumin.*, in press, DOI:10.1016/j.jlumin.2010.09.023.
(18) Pal, S.; De, G. *Mater. Res. Bull.* **2009**, *44*, 355–359.
(19) Tanahashi, I.; Yoshida, M.; Manabe, Y.; Tohda, T. *J. Mater. Res.* **1995**, *10*, 362–365.
(20) Alexandrov, A.; Smirnova, L.; Yakimovich, N.; Sapogova, N.; Soustov, L.; Kirsanov, A.; Bityurin, N. *Appl. Surf. Sci.* **2005**, *248*, 181–184.
(21) Kox, M. H. F.; Stavitski, E.; Weckhuysen, B. M. *Angew. Chem.* **2007**, *119*, 3726–3729.
(22) Jiménez, J. A.; Sendova, M.; Hartsfield, T.; Sendova-Vassileva, M. *Mater. Res. Bull.* **2011**, *46*, 158−165.
(23) Sendova, M.; Sendova-Vassileva, M.; Pivin, J. C.; Hofmeister, H.; Coffey, K.; Warren, A. *J. Nanosci. Nanotechnol.* **2006**, *6*, 748–755.
(24) Kreibig, U.; Vollmer, M. *Optical Properties of Metal Clusters*; Springer: Berlin, 1995.
(25) Pivin, J. C.; García, M. A.; Hofmeister, H.; Martucci, A.; Sendova-Vassileva, M.; Nikolaeva, M.; Kaitasov, O.; Llopis, J. *Eur. Phys. J. D* **2002**, *20*, 251–260.
(26) Hövel, H.; Fritz, S.; Hilgel, A.; Kreibig, U.; Vollmer, M. *Phys. Rev. B* **1993**, *48*, 18178–18188.
(27) Medda, S. K.; De, S.; De, G. *J. Mater. Chem.* **2005**, *15*, 3278–3284.
(28) Levy, Y.; Jurich, M.; Swalen, J. D. *J. Appl. Phys.* **1985**, *57*, 2601–2605.
(29) Mennig, M.; Schmitt, M.; Schmidt, H. *J. Sol−Gel Sci. Technol.* **1997**, *8*, 1035–1042.
(30) Li, W.; Seal, S.; Megan, E.; Ramsdell, J.; Scammon, K. *J. Appl. Phys.* **2003**, *93*, 9553–9561.
(31) Jiménez, J. A.; Sendova, M. , to be published.
(32) Ekimov, A. *J. Lumin.* **1996**, *70*, 1–20.
(33) Arnold, G. W.; Borders, J. A. *J. Appl. Phys.* **1977**, *48*, 1488–1496.
(34) Miotello, A.; DeMarchi, G.; Mattei, G.; Mazzoldi, P.; Quaranta, A. *Appl. Phys. A: Mater. Sci. Process.* **2000**, *70*, 415–419.
(35) Kellermann, G.; Craievich, A. F. *Phys. Rev. B* **2004**, *70*, 054106.
(36) Blondeau, J. Ph.; Catan, F.; Andreazza-Vignolle, C.; Sbai, N. *Plasmonics* **2008**, *3*, 65–71.
(37) Bi, H.; Cai, W.; Kan, C.; Zhang, L.; Martin, D.; Träger, F. *J. Appl. Phys.* **2002**, *92*, 7491–7497.
(38) Lawless, K. R. *Rep. Prog. Phys.* **1974**, *37*, 231–316.
(39) Hillenkamp, M.; Domenicantonio, G. D.; Eugster, O.; Félix, C. *Nanotechnology* **2007**, *18*, 015702.
(40) Hu, J.; Cai, W.; Zeng, H.; Li, C.; Sun, F. *J. Phys.: Condens. Matter* **2006**, *18*, 5415–5423.
(41) Gangopadhyay, P.; Kesavamoorthy, R.; Bera, S.; Magudapathy, P.; Nair, K. G. M.; Panigrahi, B. K.; Narasimhan, S. V. *Phys. Rev. Lett.* **2005**, *94*, 47403.
(42) Paje, S. E.; Llopis, J.; Villegas, M. A.; Fernández Navarro, J. M. *Appl. Phys. A: Mater. Sci. Process.* **1996**, *63*, 431–434.
(43) García, M. A.; García-Heras, M.; Cano, E.; Bastidas, J. M.; Villegas, M. A.; Montero, E.; Llopis, J.; Sada, C.; De Marchi, G.; Battaglin, G.; Mazzoldi, P. *J. Appl. Phys.* **2004**, *96*, 3737–3741.
(44) Jimenez, J. A.; Lysenko, S.; Zhang, G.; Liu, H. *J. Mater. Sci.* **2007**, *42*, 1856–1863.
(45) Henglein, A. *Chem. Rev.* **1989**, *89*, 1861–1873.
(46) Hu, J.; Cai, W.; Liu, P.; Zeng, H.; Li, Y.; Li, C. *J. Nanosci. Nanotechnol.* **2010**, *10*, 5369–5373.